Parameters estimation
of intensity decay relationships

Francesca Cella, Gaetano Zonno and Fabrizio Meroni
Istituto di Ricerca sul Rischio Sismico, C.N.R., Milano, Italy

Abstract

This paper presents a methodology that analyses a set of observed intensities and estimates the parameters of an adopted attenuation law directly using the data points. A procedure was developed to define and evaluate the equivalent radii D_i of the isoseismal lines. From these data it is possible to derive the parameters of the attenuation law. Moreover a validation procedure was developed to measure the capability of intensity decay relationships to reproduce the observed intensities. A case study of 55 earthquakes, divided into 9 subsets, of similar-attenuation zones, was analysed, using, as attenuation law, the one proposed by Grandori (1987, 1991) to estimate either the parameters for each single earthquake or the parameters of an average intensity decay relationship for the similar-attenuation zones. The calculated intensity decay relationships result in 60-70% of correctly reproduced points for most intensity data maps analysed. Analysing the similar-attenuation zones and different earthquakes simultaneously, the parameters of attenuation laws obtain results with a lower percentage of correctly reproduced points. The proposed methodology seems to be effective and suitable to reach practical results in parameters estimation of intensity decay relationships.

Key words *intensity data-points – equivalent radius – intensity decay relationships – validation criteria*

1. Introduction

In this paper we present a procedure to estimate the parameters of intensity decay relationships, obtained in the framework of a case study of 55 earthquakes investigated by the Italian Macroseismic Working Group of the National Project for Seismic Prevention (GNDT). The starting data, intensity data maps and the model of similar-attenuation zones were used for the analysis, without considering other available data on the study area (section 2).

As is known, the most important point in seismic hazard assessment is the issue of inten-

sity decay. The problem is due, not only to the scarcity and the quality of data (in fact in Italy there are rich archives of information on effects of historical earthquakes), but also to the procedures for data processing. In previous papers the parameters of several attenuation laws were evaluated, starting from the isoseismals (for a review, see Ambraseys, 1985). The choice of input data is a significant problem; in fact isoseismal maps for one event, drawn by different authors, show quite considerable differences that traduce different evaluations of the equivalent radii D_i of the isoseismals and consequently different estimates of the attenuation law's parameters (Barbano and Zonno, 1985). The aim of this research is the use of observed intensity maps as starting data. In this way the subjective criteria to draw the isoseismal maps are disregarded and an objective procedure is developed to evaluate the equivalent radii D_i of the isoseismal lines. Considering the distance X_i between the epicentre and the site

with intensity decay $\Delta I = i$ as a random variable, the empirical cumulative distribution can be calculated through the data points with the same intensity decay but with different site-epicentral distances. Those distributions are fitted through either *Weibull* or mixed *Weibull-Gamma* distributions, using maximum likelihood technique, and their mode is used in the definition of the isoseismal radius (section 3).

The next step to estimate the attenuation parameters is the choice of which attenuation law to adopt (*e.g.*, different attenuation models are available: Blake (1941), Sponheuer (1960) or Grandori *et al.* (1991), but it was beyond our research to check the most suitable one for each earthquake of the case study. To have homogeneity, only Grandori's attenuation law was adopted in this study (section 4).

This attenuation law is not able to take into account the local seismic effects but furnishes the intensity decay trend fitting as many points as possible for a given intensity. To measure the capability of intensity decay relationships to reproduce the observed intensities some criteria for a validation procedure have been developed (section 5).

The results obtained by analysing single earthquakes and their validation percentage are discussed.

In particular the analysis of the equivalent radius D_0 of the isoseismal line for maximum intensity I_0 shows that there is no evidence to assume that the intensity decay depends on the epicentral intensity I_0. Some considerations on the adopted attenuation law and on the supplied similar-attenuation zones are outlined in section 6.

The last part of the paper is concerned with the use of a validation to select the best set of attenuation parameters for a similar-attenuation zone. A comparison between the results obtained from single earthquake analysis and simultaneous earthquakes analysis is discussed for a sample zone (section 7).

2. Case study

The seismic classification of Italy is mainly based on the analysis of the effects of historical earthquakes (Petrini, 1980). Today there is

a need to revise the classification according to new information and methodologies. Currently, the Group of the National Project for Seismic Prevention (GNDT) is sponsoring national research to revise all original information, *i.e.* intensity point maps for the earthquakes even if the drawn isoseismals are already available. That leads to an upgrade of the national macroseismic data bank, from a very large amount of information on historical seismicity, from published and unpublished sources. A set of 55 intensity point maps has been selected to check some methodologies to estimate the intensity decay relationships starting directly from the observed intensities. The date of analysed earthquakes, its epicentral intensity I_0 and the amount of observations for each intensity degree (scale MCS) are represented in table I. The date and the epicentral locations identify the seismic sources for which the case study has furnished the intensity point maps. The seismic sources model comes from published papers (Scandone *et al.*, 1992; Scandone and Meletti, 1992) while the model of similar-attenuation zones was done by the Seismicity Working Group of GNDT, as a preliminary version (GNDT, 1994), assuming that each of the source zones identifies a similar-attenuation zone, and then linking some of them on the basis of considerations of similarity.

Figure 1 shows the epicentral location of the case study earthquakes identified by the date, and the seismic sources model, from which is derived the similar-attenuation zones model, which is depicted in fig. 2.

3. Procedure for equivalent radii evaluation

The n-th isoseismal is defined as the line that bounds the observations with an intensity value $n = I_0 - I_s$, where I_0 is the epicentral intensity and I_s is the observed intensity at the site, and it is drawn by experts who analyse the macroseismic field. The intensity decay with respect to the epicentral distance is expressed by $\Delta I = I_0 - j$, where $j = I_0, I_0 - 1, ..., 1$, so a site with an observed intensity I_s has a decay equal to $\Delta I = I_0 - I_s$. The equivalent radius D_i is de-

Table I. Earthquake list with membership of similar-attenuation zone, date, epicentral intensity and the amount of observations for each intensity degree. The 55 earthquakes of the case study of this table are ordered by decreasing degree of epicentral intensity, I_0, and by increasing date. The observations from degree III, even if in some cases they have been processed including lower intensity degrees.

| Zone	Date	I_0	III	IV	V	VI	VII	VIII	IX	X	XI
E	1638/03/27	XI		1	2	9 5	9 13	45 24	33 23	37 6	5
F	1693/01/11	XI				5 3	7 3	10 6	12 1	36	7
E	1857/12/16	XI	4	4 2	29 2	33 52	31 59	13 4	11	17	12
F	1627/07/30	X-XI			4 1	1	20 4	1 6	1	9 6	2
B	1703/01/14	X		2	3	5 2	23 14	8 19	34	56 2	48
H	1743/02/20	X	5	1	4	1	1 2	19 15	12	2	
E	1783/03/28	X		1	5	32 40	72 60	51 17	11 13	9 1	2
E	1805/07/26	X		6	3	25 2	92 8	43	12	15	1
A	1873/06/29	X	9 1	14 6	17 9	23 7	22 6	12 3	7 1	5	
B	1781/06/03	IX-X		2	2 1	1 6	8 17	40 17	13 25	8 4	6
E	1832/03/08	IX-X			5	1 9	11 4	9 5	8 4	6	
E	1836/04/25	IX-X		1	7	11 1	4 5	5	1 1	2 1	1
L	1887/02/23	IX-X		15 2	31 15	96 52	87 10	19	3	1 1	1
G	1911/10/15	IX-X	5	2 4	4	2	4 2	1	3	3	
B	1920/09/07	IX-X	21 4	43 9	55 18	69 34	52 16	41 38	26	2	
E	1930/07/23	IX-X	15 11	34 4	47 3	28 4	57 5	31 6	18 1	4	
F	1968/01/15	IX-X			1	37 16	50 22	16 2	2 3	2	5
E	1980/11/23	IX-X	109 32	304 35	229 10	186 22	128	53	9	6	
A	1695/02/25	IX		5 2	7 3	6 4	4 11	6 10	15		
F	1731/03/20	IX		1	3	1 4	10 11	4 3	1		
B	1741/04/24	IX	3	3 5	6 3	7 20	36 17	7 5	4	1	
C	1781/04/04	IX	2	8 1	2	8 6	15 15	6 5	2		
G	1818/02/20	IX	2	7	2	8 1	6	12	12		
D	1846/08/14	IX	12 6	9 1	7 7	7 6	15 5	3 2	2		
B	1919/06/29	IX	18 6	31 11	21 8	14	16 3	9	6		
C	1933/09/26	IX	26 1	60 4	56 7	56 8	41 9	23	3		
G	1894/08/08	VIII-IX	1	5 1	5	1	6	6 4			
E	1894/11/16	VIII-IX	8	19	26 5	31	14 16	8			
B	1904/02/24	VIII-IX	7	13 2	3	4	5	9	1 1		
E	1907/10/23	VIII-IX	7	5	3 3		5	15			
A	1928/03/27	VIII-IX	25 12	71 13	31 17	11 27	18 1	5 1	8		
C	1930/10/30	VIII-IX	46 5	20 4	11 5	28 13	39 11	12 1	1		
C	1943/10/03	VIII-IX	2 1	2	4	7 2	41 8	16 1	1 1		
E	1962/08/21	VIII-IX	20 5	32 1	21 6	32 6	19 13	29	8 3		
F	1978/04/15	VIII-IX	33 6	41 9	59 20	40 13	12 10	6			
C	1570/11/17	VIII		1	3	6 2	7 9	7 4	1		
A	1802/05/12	VIII		2	9 4	8 2	4 2	4 2	12		
F	1808/04/02	VIII	7	2	10 2	7 2	12	9	8		
B	1874/12/06	VIII	3		8 3	4	4	7	9		
A	1891/06/07	VIII	12 13	60 28	60 20	34 3	12 4	7			
C	1916/08/16	VIII	16	24	11	7 2	48 18	31			
F	1967/10/31	VIII	11	7 6	14		10	5	3		
B	1828/10/09	VII-VIII	4 5	1 2	4 2	11 12	29 9	1			
F	1875/12/06	VII-VIII	13 2	18 4	27 7	5 3	12 1	3			
B	1898/06/27	VII-VIII	15	42 18	18	17 5	3 1	2			
D	1909/08/25	VII-VIII	17 30	16 27	23 7	7 5		8			
B	1911/02/19	VII-VIII	26 7	28 6	16	9 2	10 3				
D	1927/12/26	VII-VIII	6 2	4	6 1	4	3		1		
D	1971/02/06	VII-VIII	4		8 2	6	12		1		
C	1971/07/15	VII-VIII	43 13	38 15	28 9	28 15	26 2	2	1		
B	1740/03/06	VII	2	7 1	2 1	10 5	2 1				
B	1922/12/29	VII	9 2	26 7	9 2	13 2	20				
C	1929/04/10	VII	21 7	29 5	20 3	5 4	9	1			
B	1958/06/24	VII	1 1			5	5	2			
E	1975/01/16	VII	46	19 9	23 21	25 11	19	1			
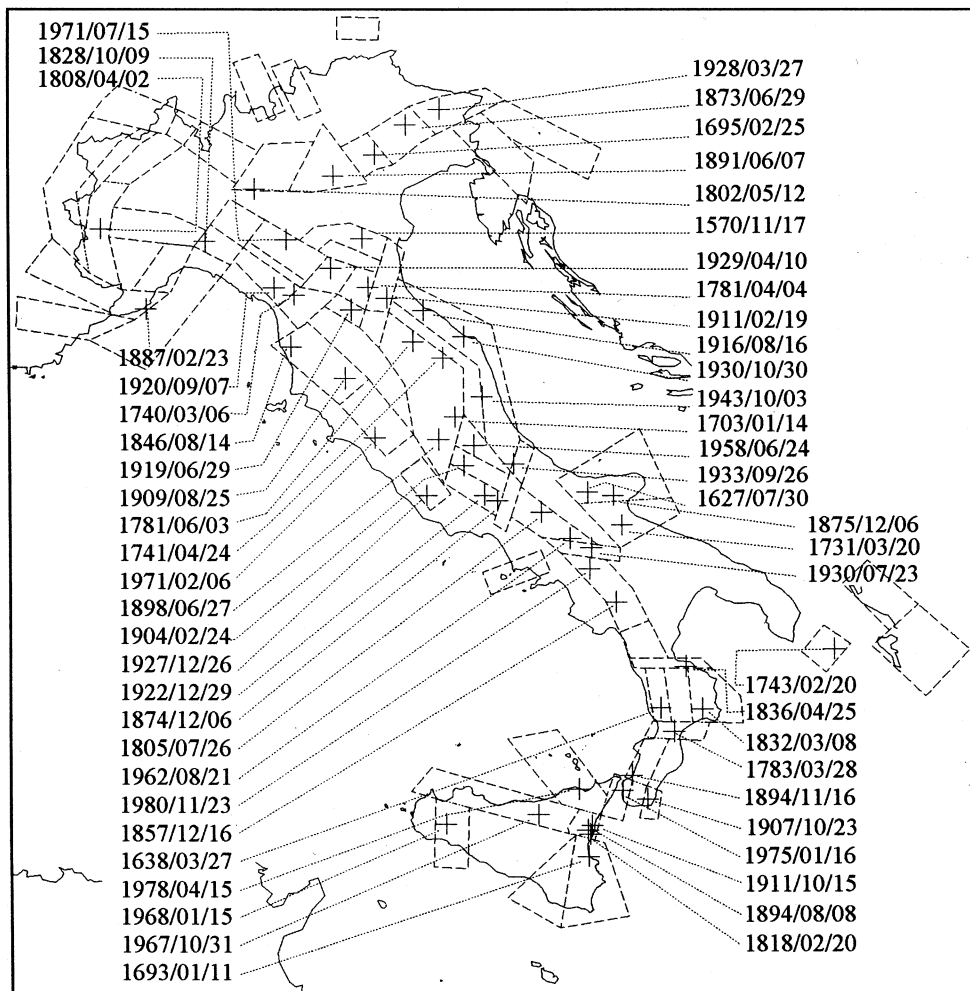
Fig. 1. Selected earthquakes, labelled by date, and source zone model used to derive the similar-attenuation zones model.

fined as the radius of the circle with an area equivalent to the one bounded by the i-th isoseismal, that is, containing the observations $\Delta I = i$. Given an earthquake of epicentral intensity $I_0 = n$, the equivalent radii D_i for the i-th isoseismal lines are obtained, with $i = 0$, $1, ..., n-1$.

Let's consider an earthquake with epicentral intensity $I_0 \geq$ VI (so as to consider 5 degrees of intensity decay), and N recorded site observa-

tions I_s. Site-epicentre distances have been grouped in S_i sets, with respect to the decay ΔI, where $\Delta I = 0, 1, ..., 5$. For a better understanding, the data forming each subset S_i are the distances $\{d_n^i\}$ between the epicentre and the sites with the same intensity decay $\Delta I = i$, where $n = 1, 2, ..., N_i$ and N_i is the total number of these sites.

Let us suppose that $\{d_n^i\}$ is a set of realisations of the distance random variable X_i. Given

each set S_i, with $i = 0, 1, ..., 5$, the corresponding empirical cumulative distribution for X_i was calculated. Non-parametric distributions were avoided because, if the data allow us to make such a choice, then that makes the inference process more accurate.

In this work, after several tests on the available data, we decided to use a Weibull or a Weibull-Gamma mixture distribution given by:

Weibull $\qquad f_\tau(x) = a\rho\,(\rho x)^{a-1}\,e^{-(\rho x)^a}$

Weibull-Gamma

$$f_\tau(x) = p a_w \rho_w\,(\rho_w x)^{a_w - 1}\,e^{-(\rho_w x)^{a_w}} +$$

$$+ (1 - p)\,\frac{\rho_\Gamma^{a_\Gamma} x^{a_\Gamma - 1}\,e^{-\rho_\Gamma x}}{\Gamma(a)}.$$
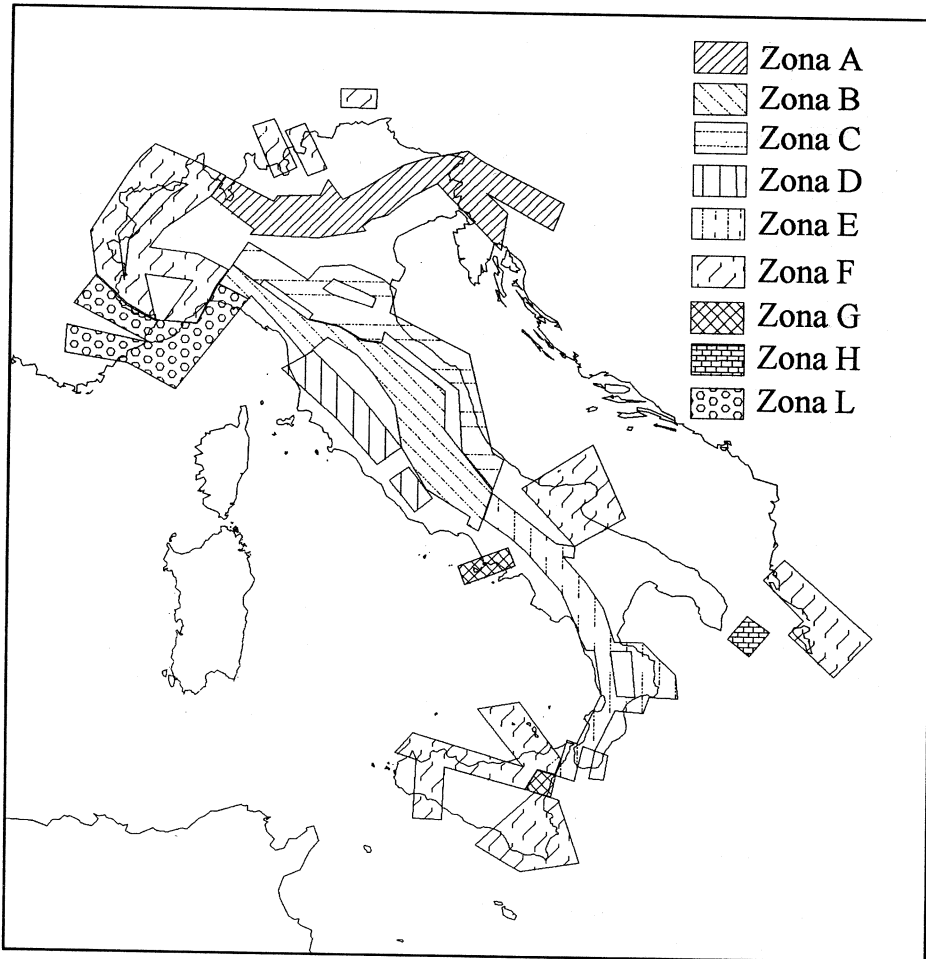

Fig. 2. Similar-attenuation zones model (GNDT, 1994, personal communication). This model is based on a modified source zones definition (Scandone *et al.*, 1992). It is assumed that each source zone is a similar-attenuation zone too. The similar-attenuation zones model was obtained grouping source zones that have similar characteristics by Gruppo di Lavoro Sismicità GNDT.

At first, we thought of using an exponential form to describe the trend of X_0 because the probability of X_0 decreases as the value of X_0 increases. Going from X_0 to X_i, with $i > 0$, it is necessary to add flexibility to the exponential distribution. The Weibull and mostly the Weibull-Gamma distribution provide just such an extra flexibility needed to make the model accurate. Moreover, the explicit form of their cumulative distribution functions makes them especially suitable if one wishes to evaluate the quantiles (Johnson and Kotz, 1970). The mode value $\hat{X}_i$ was chosen as estimate of the distance X_i, because it is representative of the greatest concentration of observations and is less affected by the outlier observations than the mean or the quantiles are. Unfortunately, to approximate the parameters of the Weibull-Gamma distribution a large number of observations is necessary, so it was decided to adopt the Weibull distribution for X_0, because of the generally small set of data in S_0, and the Weibull-Gamma mixture for the other distances X_i.

Now, let us define the equivalent radius D_i of i-th isoseismal as:

$$D_i = (\hat{X}_{i+1} - \hat{X}_i) * PK + \hat{X}_i \qquad i = 0, 1, \ldots, 4$$

(3.1)

where PK is a constant. We note that setting $PK = 0.5$ corresponds to define the equivalent radius as the arithmetic mean between the values $\hat{X}_i$ and $\hat{X}_{i+1}$. In fact D_i should be the distance where the probability of having $\Delta I = i$ is the same as that having $\Delta I = i + 1$. As we will explain in the following, we adopted the mean to treat the uncertainty of data more easily.

Some assumptions should be stated on the proposed procedure and for this purpose it is necessary to refer to table I.

First consideration: a doubtful intensity value is assigned to several earthquakes among those listed in table I (*i.e.*, $I_0 = $ IX-X). In these cases the minimum value of epicentral intensity was used in the subsequent elaboration.

Second consideration: as shown in table I, also for the site intensity observations several cases of uncertain assignment are present. In those situations we decided to adopt an operative procedure which considers the two values

as equiprobable. Based on the difficulty of considering all the possible combinations of such values, the procedure for equivalent radius estimation was modified: for the definition of the five data sets $\{d_n^i\}$, the uncertain data (*i.e.*, $I_s = $ VIII-IX) were considered twice, first considering smaller degree ($I_s = $ VIII, below procedure), and then larger degree ($I_s = $ IX above procedure). So two different data sets are produced $\{d_n^i\}'$, $\{d_n^i\}''$ and, for them, the corresponding modes $(\hat{X}_i)'$ and $(\hat{X}_i)''$ are evaluated.

Now the mode $\hat{X}_i$ is redefined as follows:

$$\hat{X}_i = \frac{(\hat{X}_i)' + (\hat{X}_i)''}{2} \qquad (3.2)$$

The last assumption concerns the observed intensities larger than the epicentral intensity I_0 (see table I): we always substituted such intensities with the epicentral intensity because it is not possible to take into account the local effects.

3.1. *Case study: equivalent radii evaluation*

The described procedure was applied to evaluate the equivalent radii of isoseismal lines for each earthquake of the case study. As an example, for a better explanation of the procedure, the application to the 27 March 1928 earthquake will be analysed in detail. This earthquake has an epicentral intensity I_0 equal to VIII-IX (MCS) but in the analysis it will be considered as $I_0 = $ VIII. The observed intensities equal to IX and to VIII-IX (9 sites, table I) are greater than the assumed epicentral intensity ($I_0 = $ VIII) and they will be considered as VIII. The existence of many observed intensities that are classified with two degrees of scale MCS, *i.e.* 27 sites with $I_s = $ VI-VIII, shows the necessity to consider the uncertain data through the relation (3.2). It means that two empirical data sets $\{d_n^i\}'$ and $\{d_n^i\}''$ have to be formed considering all the doubtful observed intensity I_s respectively as either the below or the above degree. The two empirical data sets and their cumulative distributions $F(X_i)'$, $F(X_i)''$ versus the distance are shown (fig. 3)
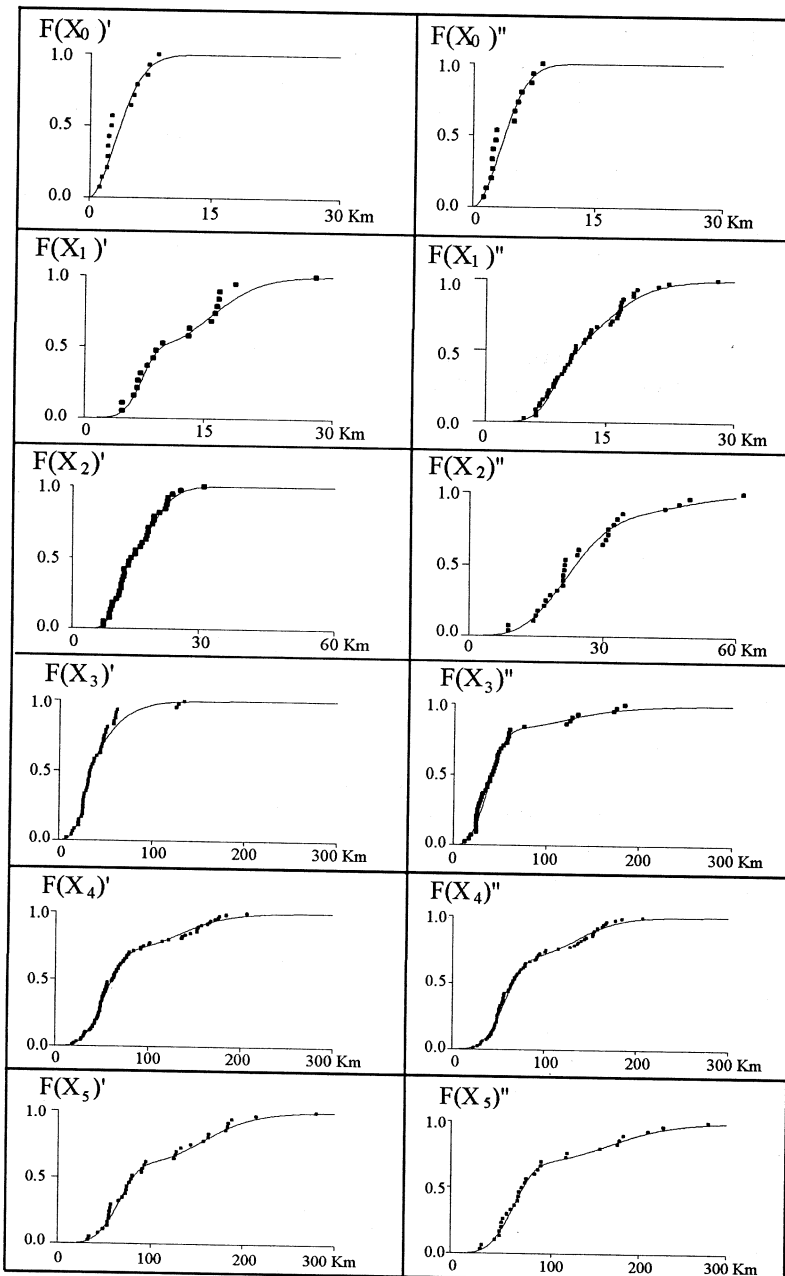
Fig. 3. Empirical data (dots) and cumulative distributions (solid line) *versus* distance of all the intensity decay analysed (X_i, $i = \Delta I = 0, 1, ..., 5$) for the 27 March 1928 earthquake are shown. On the left of the figure, the cumulative distributions (single apex) are obtained with the below procedure, on the right (double apex) with the above procedure. The Weibull function is used to estimate X_0 and Weibull-Gamma mixture to estimate the other X_i.

for all the analysed intensity decays X_i, $i = \Delta I = 0, 1, ..., 5$. The parameters of the Weibull and Weibull-Gamma distributions were evaluated through maximum likelihood technique. After several tests on the available data, we adopted, as general rule, the Weibull function to estimate X_0 and Weibull-Gamma mixture to estimate the other X_i. In fact, even if this is not the case, analysing other earthquakes we often

found that there were a very few data to estimate X_0 and it was very difficult to estimate the parameters for a Weibull-Gamma mixture, so it was decided that the use of the Weibull distribution was more appropriate. We note that the large number of uncertain observations change the cumulative distribution. A good evidence of this behaviour is shown in fig. 4, where in each frame the two densities of prob-
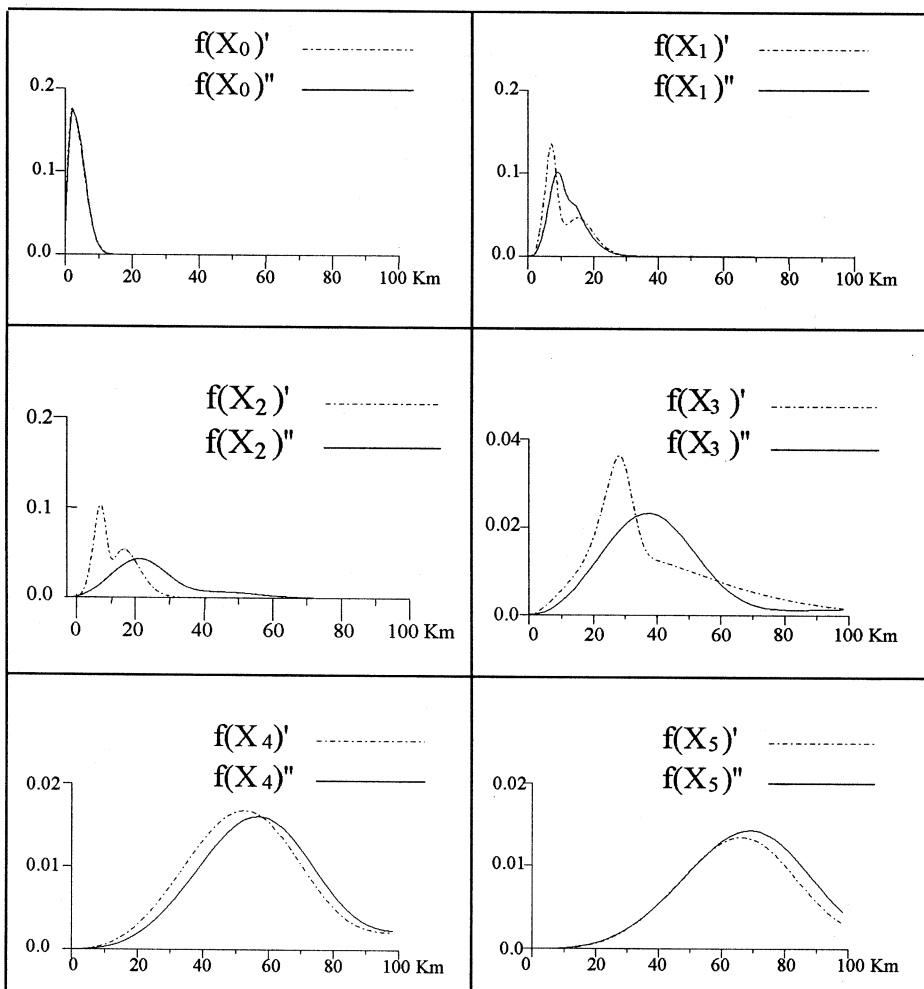

Fig. 4. Probability densities *versus* distance of all the intensity decay analysed (X_i, $i = \Delta I = 0, 1, ..., 5$) for the 27 March 1928 earthquake are shown. The graphs with dashed line and solid line represent the below and above procedure respectively. The mode value about below and above procedure disagrees when there are a large number of uncertain observations.

Table II. Mode values X_0, X_1, X_2, X_3 and X_4 (relation (3.2)), calculated for 51 earthquakes listed by similar-attenuation zone, and by decreasing degree of epicentral intensity I_0. Earthquakes are also labelled by numbers.

Zone	No.	Date	I_0	$\hat{X}_0$	$\hat{X}_1$	$\hat{X}_2$	$\hat{X}_3$	$\hat{X}_4$	$\hat{X}_5$
A	1	1873/06/29	10	0.1	4.9	7.2	16.0	62.7	61.3
A	2	1695/02/25	9	4.0	8.3	17.7	88.1	110.1	98.4
A	3	1928/03/27	8-9	3.0	8.1	15.7	33.1	54.9	67.8
A	4	1802/05/12	8	4.6	13.4	20.3	45.4	107.8	
A	5	1891/06/07	8	2.0	8.0	15.1	29.8	84.6	158.4
B	6	1703/01/14	10	11.8	13.9	33.9	41.8	78.7	155.5
B	7	1781/06/03	9-10	5.0	10.0	15.9	50.6	54.3	91.5
B	8	1920/09/07	9-10	4.1	15.2	26.2	49.2	93.2	167.7
B	9	1741/04/24	9	8.4	18.5	28.9	37.8	55.9	121.2
B	10	1919/06/29	9	1.9	7.8	14.2	28.0	44.0	68.6
B	11	1904/02/24	8-9	3.4	7.7	19.5	19.0	45.0	60.3
B	12	1874/12/06	8	7.5	19.4	28.1	62.1	92.4	75.3
B	13	1828/10/09	7-8	15.3	21.8	94.0	112.9	150.2	159.6
B	14	1898/06/27	7-8	4.1	15.4	25.1	73.3	56.3	132.8
B	15	1911/02/19	7-8	7.3	23.2	35.2	54.5	72.8	104.6
B	16	1740/03/06	7	7.5	18.4	18.2	41.1	110.6	
B	17	1922/12/29	7	11.8	22.3	43.4	44.4	88.0	88.8
C	18	1781/04/04	9	4.1	5.6	10.2	13.7	40.9	70.5
C	19	1933/09/26	9	10.2	16.5	23.9	39.2	57.8	99.6
C	20	1930/10/30	8-9	13.9	11.9	35.6	72.3	124.4	178.5
C	21	1943/10/03	8-9	7.7	18.8	32.6	53.4	94.9	141.2
C	22	1570/11/17	8	6.1	8.9	10.4	45.6	68.7	
C	23	1916/08/16	8	4.3	6.1	23.6	108.2	88.2	157.6
C	24	1971/07/15	7-8	11.3	20.9	55.2	92.6	115.0	
C	25	1929/04/10	7	4.7	9.8	28.5	83.4	107.3	151.0
D	26	1846/08/14	9	0.4	6.2	9.4	11.3	20.4	33.2
D	27	1909/08/25	7-8	10.0	21.6	35.7	63.6	79.3	81.1
D	28	1927/12/26	7-8	2.5	4.5	15.4	26.9	40.9	45.1
D	29	1971/02/06	7-8	0.1	15.2	25.9	34.8	35.6	57.8
E	30	1638/03/27	11	3.9	11.7	24.1	33.6	67.8	92.9
E	31	1857/12/16	11	19.8	16.9	24.4	45.3	55.7	75.1
E	32	1783/03/28	10	7.3	15.3	32.1	54.4	89.0	95.5
E	33	1805/07/26	10	8.7	12.7	28.4	45.5	86.2	116.9
E	34	1832/03/08	9-10	10.7	20.3	30.0	47.3	91.3	
E	35	1836/04/25	9-10	7.1	11.8	26.6	47.7	60.1	
E	36	1930/07/23	9-10	11.7	30.7	50.9	75.5	102.1	172.3
E	37	1980/11/23	9-10	5.6	27.4	52.2	75.2	140.8	236.5
E	38	1894/11/16	8-9	3.4	17.9	44.0	95.2	132.6	171.6
E	39	1907/10/23	8-9	10.2	25.0	51.5	50.9	88.8	129.2
E	40	1962/08/21	8-9	15.9	35.1	58.0	81.9	109.6	133.6
E	41	1975/01/16	7	6.2	14.2	31.3	49.5	59.9	72.9
F	43	1693/01/11	11	19.3	31.7	48.2	59.6	93.6	107.2
F	42	1627/07/30	10-11	10.4	23.1	34.7	60.4		120.8
F	44	1968/01/15	9-10	6.9	19.2	36.3	54.3	94.8	
F	45	1731/03/20	9	15.1	34.6	56.3	109.3	168.5	
F	46	1978/04/15	8-9	12.2	18.7	36.3	69.5	100.1	110.4
F	47	1808/04/02	8	4.0	8.2	19.5	55.5	82.9	165.2
F	48	1967/10/31	8	11.2	15.9	27.5	48.1	72.3	92.2
G	49	1818/02/20	9	0.3	5.9	15.6	15.2	46.6	73.0
G	50	1894/08/08	8-9	0.6	4.4		6.2	17.8	
L	51	1887/02/23	9-10	7.5	13.6	21.0	48.5	98.7	

Table III. Final results of single earthquake analysis. Data sets are identified by event number (see table II). Equivalent radii D_0, D_1, D_2, D_3 and D_4, Grandori's attenuation law parameters Ψ, Ψ_0 and D_0 and results of categories percentage (E, O, U, $O+$, $U+$) of the validation procedure are listed.

Zone	No.	I_0	D_0	D_1	D_2	D_3	D_4	Ψ	Ψ_0	D_0	$E\%$	$O\%$	$U\%$	$O+\%$	$U+\%$
A	1	10	2.5	6.1	11.6	89.4	86.1	2.8	1.4	2.5	57.0	12.8	22.1	4.7	3.5
A	2	9	6.2	13.0	52.9	99.1	121.1	2.5	1.1	6.2	50.0		37.5		12.5
A	3	8-9	5.5	11.9	24.4	44.0	61.3	1.5	1.1	5.5	74.6	2.8	21.1		1.4
A	4	8	9.0	16.8	32.8	76.6	139.0	2.1	0.9	9.0	95.8	4.2			
A	5	8	5.0	11.5	22.4	57.2	121.5	2.2	1.3	5.0	78.3	8.3	8.3	1.7	3.3
B	6	10	12.9	23.9	37.8	60.2	117.1	1.8	0.9	12.9	50.0	20.1	19.1	2.5	8.3
B	7	9-10	7.5	13.0	33.2	52.4	72.9	1.9	0.7	7.5	58.0	5.1	30.4		6.5
B	8	9-10	9.6	20.7	37.7	71.2	130.4	1.8	1.1	9.6	62.2	13.3	18.7	4.3	1.4
B	9	9	13.4	23.7	33.4	46.9	88.6	1.8	0.8	13.4	58.3	18.8	11.5	8.3	3.1
B	10	9	4.8	11.0	21.1	36.0	56.3	1.5	1.3	4.8	56.3	6.3	22.9	2.1	12.5
B	11	8-9	5.6	13.6	25.2	32.0	52.6	1.7	1.5	5.6	75.0	15.0	10.0		
B	12	8	13.5	23.8	45.1	77.3	107.6	1.5	0.8	13.4	65.0	5.0	20.0	5.0	5.0
B	13	7-8	18.5	57.9	103.5	131.6	154.9	0.9	2.1	18.5	69.4	1.6	29.0		
B	14	7-8	9.7	20.2	49.2	88.9	94.6	1.4	1.1	9.7	67.9	3.6	28.6		
B	15	7-8	15.2	29.2	44.8	63.6	88.7	1.2	0.9	15.2	75.0	4.2	16.7		4.2
B	16	7	13.0	23.7	29.6	75.9	145.4	3.3	0.8	12.9	61.1	11.1	27.8		
B	17	7	17.0	32.8	43.9	66.2	88.4	1.2	0.9	17.0	65.7	8.6	22.9		2.9
C	18	9	4.8	7.9	11.9	27.3	55.7	2.3	0.6	4.8	64.9	17.5	8.8	5.3	3.5
C	19	9	13.3	20.2	31.5	48.5	78.7	1.6	0.5	13.3	60.7	26.4	11.4	1.4	
C	20	8-9	12.9	23.7	54.0	98.3	151.4	1.8	0.8	12.9	46.2	14.4	29.8	1.9	7.7
C	21	8-9	13.2	25.7	43.0	74.2	118.0	1.5	0.9	13.2	57.9	18.4	21.1		2.6
C	22	8	7.5	9.6	28.0	57.1	80.2	3.7	0.3	7.5	35.7	10.7	42.9	3.6	7.1
C	23	8	5.2	14.9	65.9	140.5	122.9	4.6	1.9	5.2	55.7	3.8	36.8		3.8
C	24	7-8	16.1	38.1	73.9	103.8	126.2	1.1	1.4	16.1	57.5	9.6	28.8		4.1
C	25	7	7.2	19.1	55.9	95.3	129.1	1.7	1.6	7.2	73.7	10.5	15.8		
D	26	9	3.3	7.8	10.3	15.8	26.8	1.6	1.4	3.3	62.5	15.0	12.5	2.5	7.5
D	27	7-8	15.8	28.6	49.6	71.4	80.2	1	0.8	15.8	60.0	5.0	30.0		5.0
D	28	7-8	3.5	9.9	21.1	33.9	43.0	1.2	1.9	3.5	62.5	12.5	25.0		
D	29	7-8	7.7	20.5	30.3	35.2	46.7	1.2	1.7	7.7	76.9	7.7	15.4		
E	30	11	7.8	17.9	28.9	50.7	80.4	1.5	1.3	7.8	58.4	23.0	14.8	1.9	1.9
E	31	11	18.4	20.7	34.9	50.5	65.4	2.7	0.1	18.4	56.0	17.2	9.9	9.1	7.8
E	32	10	11.3	23.7	43.3	71.7	92.3	1.3	1.1	11.3	51.9	14.3	26.9	0.6	6.2
E	33	10	10.7	20.6	36.9	65.8	101.5	1.5	0.9	10.7	48.0	16.7	28.3	4.0	3.0
E	34	9-10	15.5	25.1	38.7	69.3	113.3	1.7	0.6	15.4	68.1	10.6	12.8	2.1	6.4
E	35	9-10	9.5	19.2	37.1	53.9	66.3	1.2	1	9.4	58.6	10.3	24.1		6.9
E	36	9-10	21.2	40.8	63.2	88.8	137.2	1.4	0.9	21.2	57.1	20.1	18.8	3.2	0.6
E	37	9-10	16.5	39.8	63.7	108.0	188.7	1.6	1.4	16.5	55.2	29.2	9.7	5.9	
E	38	8-9	10.6	30.9	69.6	113.9	152.1	1.3	1.9	10.6	73.9	1.4	18.8		5.8
E	39	8-9	17.6	38.2	64.4	69.9	109.0	2.9	1.2	17.6	100.0				
E	40	8-9	25.5	46.5	69.9	95.7	121.6	1.1	0.8	25.5	66.4	8.2	21.8	1.8	1.8
E	41	7	10.2	22.8	40.4	54.7	66.4	1	1.2	10.2	78.6	3.6	16.1		1.8
F	42	11	25.5	39.9	53.9	76.6	100.4	1.2	0.6	25.5	54.4	22.2	15.6	2.2	5.6
F	43	10-11	16.8	28.9	47.5	43.0	60.4	1.5	0.7	16.8	64.0	14.0	20.0		2.0
F	44	9-10	13.0	27.7	45.3	74.5	115.0	1.4	1.1	13.0	68.6	27.5	2.0	2.0	
F	45	9	24.8	45.5	82.8	138.9	198.1	1.5	0.8	24.8	60.0	17.1	17.1		5.7
F	46	8-9	15.4	27.5	52.9	84.8	105.2	1.3	0.8	15.4	60.5	18.5	18.5		2.5
F	47	8	6.1	13.8	37.5	69.2	124.1	2	1.3	6.1	65.5	20.7	13.8		
F	48	8	13.5	21.7	37.8	60.2	82.2	1.5	0.6	13.5	100.0				
G	49	9	3.1	10.7	20.2	30.9	59.8	1.7	2.5	3.1	46.2	15.4	28.2	5.1	5.1
G	50	8-9	2.5	4.1	3.1	12.0	23.6	1.3	0.6	2.5	52.9	5.9	35.3		5.9
L	51	9-10	10.6	17.3	34.8	73.6		2.41	0.64	10.6	43.3	14.9	25.4	3.4	13.1

ability $f(X_i)'$, $f(X_i)''$ vs. the distance are shown. The mode value X_i, chosen as an estimator of distance X_i, and representative of the highest concentration of observations, shows for the intensity decay $\Delta I = 2$, a mode value $(\hat{X}_2)' = 10$ km (below procedure) and a mode value $(\hat{X}_2)'' = 21.3$ km (above procedure). The final mode value is obtained as the mean (relation (3.2)) of two values and is $\hat{X}_2 = 15.7$ km (earthquake No. 3, table II).

The Weibull-Gamma mixture distribution has a bimodal trend (fig. 4), and between two local maxima as automatic procedure we always select the greater one. Using the same procedure all the values $\hat{X}_i$, $i = 0, 1, ..., 5$ are evaluated. At least it is possible to evaluate the equivalent radii D_0, D_1, D_2, D_3 and D_4 through the relation (3.1), assuming $PK = 0.5$ (table III).

It becomes clear that the estimation of $\hat{X}_i$ is the critical point of the analysis. The 27 March 1928 earthquake, chosen as an example to illustrate the procedure, has a large amount of data for each intensity degree and did not raise problems. Other earthquakes, with a poor set of data, furnished not reasonable estimates, and in such cases it was necessary to leave the automatic procedure and to activate further analysis. In the following we present some cases where it was not possible to reach a good evaluation of the equivalent radii:

– 1743/02/20 with $I_0 = X$, located in the Otranto channel (H Zone). It presents many problems, such as the two highest observations located much more distant from the epicentre than the lower ones and it caused the definition of incongruent equivalent radii. This intensity data set was not considered in any situation during the analysis.

– 1875/12/06 with $I_0 = $ VII-VIII, located in the Foggia neighbourhood, at S. Marco in Lamis (F Zone). The analysis of this earthquake leads to the definition of very large equivalent radii, probably due to an underestimated epicentral intensity. This event was analysed only alone, it was not included in the subsequent analysis of similar-attenuation zones.

– 1911/10/15 with $I_0 = $ IX-X, located in Etna zone (G Zone). This earthquake shows very small equivalent radii D_3, D_4 and D_5 and

it caused problems in the analysis with other events of the zone. This intensity data set was excluded in all situations.

– 1958/06/24 with $I_0 = $ VII, located in Aquilano, in B Zone, that has too few data (table I, one before the last). Also this intensity data set was not used for the analysis.

Table II reports the mode values $\hat{X}_0$, $\hat{X}_1$, $\hat{X}_2$, $\hat{X}_3$, $\hat{X}_4$ and $\hat{X}_5$ (relation (3.2)) calculated for 51 earthquakes while the equivalent radii D_0, D_1, D_2, D_3 and D_4 are shown in table III.

4. Adopted attenuation law

Starting from the equivalent radii of the isoseismal lines evaluated in the previous section, we chose between different attenuation laws (i.e., Blake, Sponheuer, Exponential, Grandori) for parameters estimation of intensity decay relationships. Grandori's attenuation law in this study was adopted a priori because it has interesting properties: a good description of intensity decay for sites near the earthquake source, usually underestimated; a unique attenuation law with few coefficients, that makes the intensity decay dependent on the epicentral intensity I_0, when the historical data show this kind of behaviour, instead of a relation with different coefficients for each intensity I_0.

This law was chosen in previous papers (Grandori et al., 1987, 1991; Petrini, 1995; Teramo, 1995), as flexible and efficacious for a good description of the intensity decay relationship and more suitable for seismic hazard assessment.

We chose a unique attenuation model, suitable to estimate the attenuation parameters of intensity decay relationships analysing either each single earthquake or simultaneously more earthquakes. The structure of the attenuation law proposed by Grandori is given by the following relations:

$$I_0 - i = \frac{1}{\ln \Psi} \ln \left[1 + \frac{\Psi - 1}{\Psi_0} \left(\frac{D_i}{D_0} - 1 \right) \right] \qquad (4.1)$$

$$\Phi = \frac{D_0 \, (I_0 = J)}{D_0 \, (I_0 = J - 1)} \qquad (4.2)$$

1105

$$\Psi_0 = \frac{(D_1 - D_0)}{D_0} \qquad \Psi_n = \frac{(D_{n+1} - D_n)}{D_n - D_{n-1}}$$

$$\Psi = \text{mean}(\Psi_1, \Psi_2, \ldots, \Psi_n) \qquad (4.3)$$

where D_0 is the equivalent radius of the isoseismal line of the maximum intensity I_0; D_i is the equivalent radius of the isoseismal line of intensity $I = I_0 - i$; Ψ and Ψ_0 are parameters.

As mentioned, the characteristics of the relation (4.1) is that the intensity decay depends on the epicentral intensity I_0 by means of D_0 and of the relation (4.2). Let us observe that the attenuation is faster for weak earthquakes when $\Phi > 1$ and faster for strong earthquakes when $\Phi < 1$, whereas it is constant for all the intensities if $\Phi = 1$. The parameter Φ can be evaluated if there is a monotonic relation between the values of D_0 and the epicentral intensities I_0 when more earthquakes of the same similar-attenuation zone and with different epicentral intensity I_0 are simultaneously analysed. The functional structure (4.1) is used as an isotropic model but an azimuth factor could be introduced through the equivalent radius D_0. In this paper we neglect the possible directional effect of intensity decay.

5. Validation procedure

To yield a measure of the capability of intensity decay relationship in reproducing the observed intensities, some criteria for a validation procedure were developed. The attenuation law furnishes, through the estimated parameters, and for a site at a certain distance, a value of intensity that has to be compared with the real observed intensity. For this purpose it is necessary to define some ranges that classify the match between the observed and the calculated intensity:

$E = Equal$: match between observed and calculated intensity;

$O = Overestimation$ of *one* degree of observed intensity;

$U = Underestimation$ of *one* degree of observed intensity;

$O+ = Overestimation$ of *more than one* degree of observed intensity;

$U+ = Underestimation$ of *more than one* degree of observed intensity.

Some assumptions were established:

– the calculated intensity could never match the uncertain observations (*i.e.*, I_s = VI-VII) but if the attenuation law furnishes either I_s = VI or I_s = VII we assume it in category E;

– the observed intensities greater than epicentral intensity are counted in category E or U depending on whether they are uncertain observations or not;

– the validation is done only for the observed intensities $I_s \geq$ VI, considering that in MCS scale VI is the minimum degree indicating a damage to buildings.

A percentage of each class on the number of the analysed data points gives a measure of the goodness of the estimated intensity decay relationship (table III and table V).

6. Analysis of single earthquakes

The first result of this work was a detailed analysis of the 55 considered earthquakes and the definition of an attenuation law for 51 of them (section 3.1). So the calculated attenuation law is here described for every single earthquake.

A summary of the gained results is shown in table III, in which data sets have been grouped for every zone and sorted on epicentral intensity. The data set was named only with the label number, the same as in table II, to save space. It is stressed that the results were obtained using $PK = 0.5$ in (3.1). The table contains the D_i sets, with $i = 0, 1, \ldots, 4$, the Ψ, Ψ_0, and D_0 parameters from Grandori's attenuation function, and the validation of results for every set of parameters, expressed through the percentage of the classes described in section 5.

In general the results gave a weighted average of 58.2% of exact observations (E) on the number of observations of each event. There was a maximum of more than 90% for the extreme regular earthquakes (well fitted by an isotropic model), and results lower than 40% for the situations most critical to model. The average of the *underestimated* observations of

Table IV. The 10 sets of equivalent radii, Grandori's attenuation law parameters and percentage of validation procedure obtained for B zone. The best results are obtained with a *PK* value of 0.8.

Zone	PK	D_0	D_1	D_2	D_3	D_4	Ψ	Ψ_0	D_0	E%	O%	U%	O+%	U+%
	0.1	8.2	17.7	33.8	54.0	82.5	1.45	1.16	8.2	45.7	10.0	30.4	2.2	11.7
	0.2	9.1	19.3	35.7	56.9	85.4	1.42	1.12	9.1	49.5	11.8	26.6	2.3	9.8
	0.3	10.0	20.8	37.7	59.7	88.4	1.39	1.09	10.0	50.3	13.9	25.3	2.6	7.9
	0.4	10.8	22.4	39.6	62.5	91.4	1.36	1.07	10.8	52.1	15.2	23.3	3.1	6.3
B	0.5	11.7	24.0	41.5	65.4	94.3	1.33	1.05	11.7	52.8	17.0	21.2	3.6	5.4
	0.6	12.6	25.6	43.5	68.2	97.3	1.31	1.03	12.6	53.7	18.2	18.4	4.8	4.8
	0.7	13.5	27.1	45.4	71.0	100.2	1.29	1.01	13.5	54.4	19.6	16.0	6.0	4.1
	0.8	14.4	28.7	47.3	73.8	103.2	1.28	1.00	14.4	54.7	21.0	13.8	6.8	3.7
	0.9	15.2	30.3	49.3	76.7	106.2	1.26	0.99	15.2	53.1	23.2	12.8	7.8	3.1
	1.0	16.1	31.9	51.2	79.5	109.1	1.25	0.98	16.1	52.7	24.4	11.7	9.0	2.2

Table V. Final results of similar-attenuation zones analysis. Equivalent radii, Grandori's attenuation law parameters and percentage of validation procedure obtained for all the analysed zones. The *PK* value identifies the set of attenuation parameters that best reproduce the observations for each zone.

Zone	PK	D_0	D_1	D_2	D_3	D_4	Ψ	Ψ_0	D_0	E%	O%	U%	O+%	U+%
A	0.9	8.0	14.5	39.7	79.8	95.2	2.0	0.8	8.0	55.6	19.9	11.4	6.4	6.7
B	0.8	14.4	28.7	47.3	73.8	103.2	1.3	1.0	14.4	54.7	21.0	13.8	6.8	3.7
C	0.6	10.5	21.4	49.1	78.5	115.2	1.6	1.0	10.5	50.9	20.2	18.1	3.3	7.5
D	1.0	11.9	21.6	34.1	44.0	54.3	1.0	0.8	11.9	37.0	23.5	9.9	24.7	4.9
E	0.6	15.6	30.6	50.5	77.8	115.0	1.4	1.0	15.6	47.3	21.4	18.8	8.0	4.5
F	0.9	20.6	35.4	59.3	92.6	116.8	1.2	0.7	20.6	52.6	29.1	10.4	4.4	3.5
G	1.0	4.1	9.3	14.3	23.1	42.4	1.6	1.2	4.1	52.1	15.5	14.1	9.9	8.5
L	0.9	13.0	20.3	45.8	93.7		2.7	0.6	13.0	48.9	16.4	19.8	7.1	7.8

one degree (*U*), equal to 19.4%, was greater than the *overestimated* ones of one degree (*O*), 15.57%.

Reproduction of the worst events concerned earthquakes with very close observations of different intensity (*i.e.*, 1887/02/23 No. 51 of L zone) or with a very small set of observations for certain D_i (*i.e.*, 1570/11/17 No. 22 of C zone) and, as stressed in paragraph 3.1, in such cases it should be better to activate further analysis and a manual controlled procedure. Otherwise the best reproduced events had

a low I_0, about VIII or VIII-IX, so not a large number of observations (I_s = VI or I_s = VII) were considered.

6.1. *Discussion on the intensity decay shapes*

Some considerations on the intensity decay relation used are required. An important feature of the Grandori relationship is the possibility to model the intensity decay according to the epicentral intensity. This feature is repre-

sented by Φ parameter and it is defined by the ratio between D_0 of different epicentral intensity (relation (3.2)) but, considering all the earthquakes of the same similar-attenuation zones, no monotonic relations were detected between the epicentral intensities I_0 and the value of equivalent radii D_0. This can be seen in table III analysing the D_0 and I_0 columns and also, with a graphic representation, in fig. 5. In this figure D_0 stands for the analysed
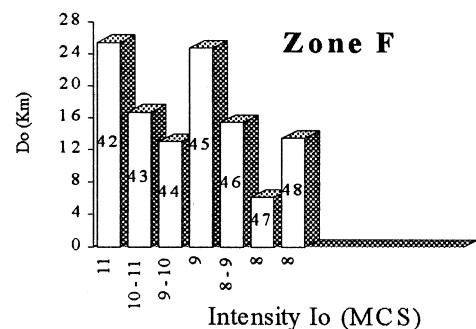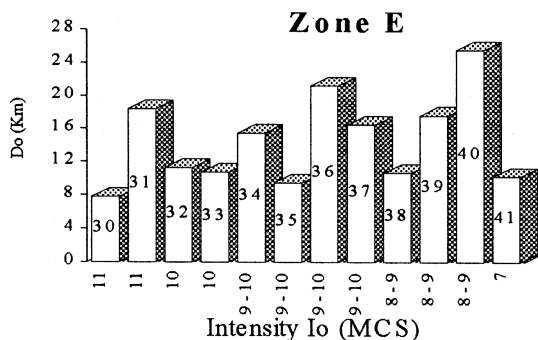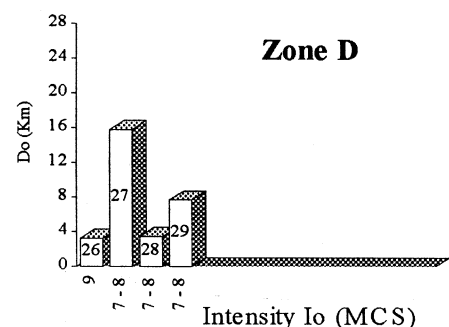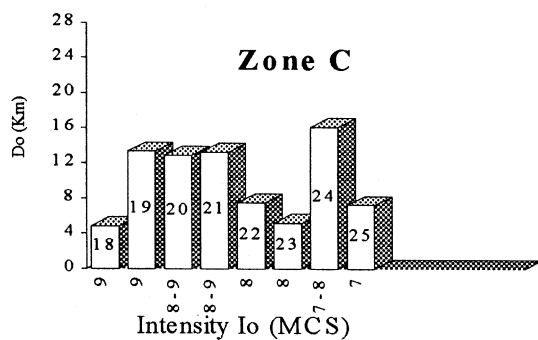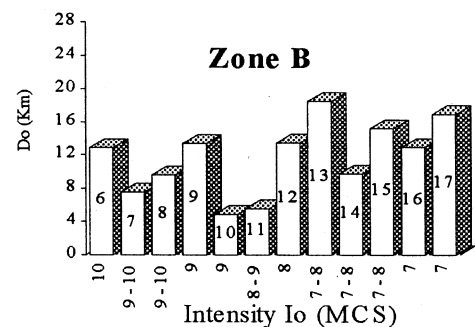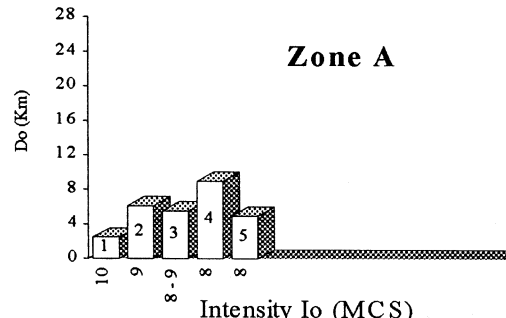
Fig. 5. Equivalent radius, D_0, and epicentral intensity, I_0, represented to evaluate their possible correlation. Only zones containing more than two earthquakes are represented.

events, grouped by zones (each column is an earthquake labelled by the identificative number) versus the epicentral intensity sorted in decreasing order. Three zones are not present in this representation, G and L zones because they have two and one earthquakes respectively, too few to find a relation between I_0 and D_0, and obviously H zone since its unique earthquake did not furnish useful radii.

A glance at this figure shows that there is no monotonic relation between I_0 and D_0 and the D_0 of events with the same I_0 are very different from each other. Thus, it was not possible to evaluate an average value of Ψ maintaining the decay dependence on the epicentral intensity I_0 through the ratio Φ of Grandori's attenuation law. At this point, for seismic hazard purposes, the choice was to use either the intensity decay relationship of the most representative earthquake or to estimate an average intensity decay considering all the earthquakes. The choice did not concern the attenuation law used, so for this reason we estimated an average intensity decay but still using Grandori's attenuation law and we used the described empirical validation procedure to examine the results as illustrated below.

7. Analysis of similar-attenuation zones

The process of analysis of the similar-attenuation zone starts again from the equivalent radii of the isoseismal lines. As seen in section 6 the *underestimated* observations on the average are greater than the *overestimated* ones. This fact suggested that the choice of $PK = 0.5$ (relation (3.1)) was not always optimal: it is reasonable to think that in many situations it proposes D_i much too small. As a consequence, different PK variables were adopted for the calculation of the parameters of similar-attenuation zones.

The procedure is the following: the mode values $\hat{X}_i$, previously estimated, are selected among the earthquakes belonging to the same similar-attenuation zone and the mean of all mode values $\hat{X}_0$, $\hat{X}_1$, $\hat{X}_2$, $\hat{X}_3$, $\hat{X}_4$ and $\hat{X}_5$ is chosen as estimate of the zone. For instance, if we

consider zone B, with 12 earthquakes, the corresponding distances (in km) of the mode value are $\hat{X}_0 = 7.3$, $\hat{X}_1 = 16.1$, $\hat{X}_2 = 31.9$, $\hat{X}_3 = 51.2$, $\hat{X}_4 = 78.4$, and $\hat{X}_5 = 111.44$. Then the equivalent radii are calculated using the relation (3.1) varying PK value, from 0.1 to 1 with a step of 0.1. Table IV shows the 10 sets of equivalent radii obtained varying PK and the corresponding parameters of the attenuation law evaluated. It can be noticed that the value D_i increases to reach a maximum of $\hat{X}_{i+1}$ (when $PK = 1$). As a consequence the values of Ψ, Ψ_0, and D_0 parameters characterising the attenuation law and its validation, obviously change. The criteria to choose the best set of parameters for seismic hazard evaluation are the following:

1) largest amount of intensity observations in E class;

2) minimum number of intensity observations in U and $U+$ classes;

3) minimum number of intensity observations in O and $O+$ classes;

4) it is better a higher percentage in class O rather than in class U.

The parameters set, selected among the proposed ones and corresponding to $PK = 0.8$, satisfy the assumed criteria.

To estimate the average parameters by the analysis of the grouped earthquakes of similar-attenuation zones, it is necessary to point out some considerations comparing all the intensity data sets together: we can analyse the results beginning from fig. 6. In this figure the equivalent radii D_i ($i = 0, 1, ..., 4$) are shown by histograms drawn for every earthquake: each bar is labelled on the X-axes by the number in table II and table III. On the Y-axes the values of the radii D_0, D_1, ..., D_4 are represented in kilometres. On the background, in grey, the global value obtained for each zone is shown. With the aid of these graphs, for every D_i it is possible to have an overview of the earthquake equivalent radii dimension in comparison with the radii computed for the zones. It is supposed that these events are characteristics for the zones and they describe the zone average trend. In the present situation it seems that some earthquakes of the same zone have different attenuation characteristics. Using this
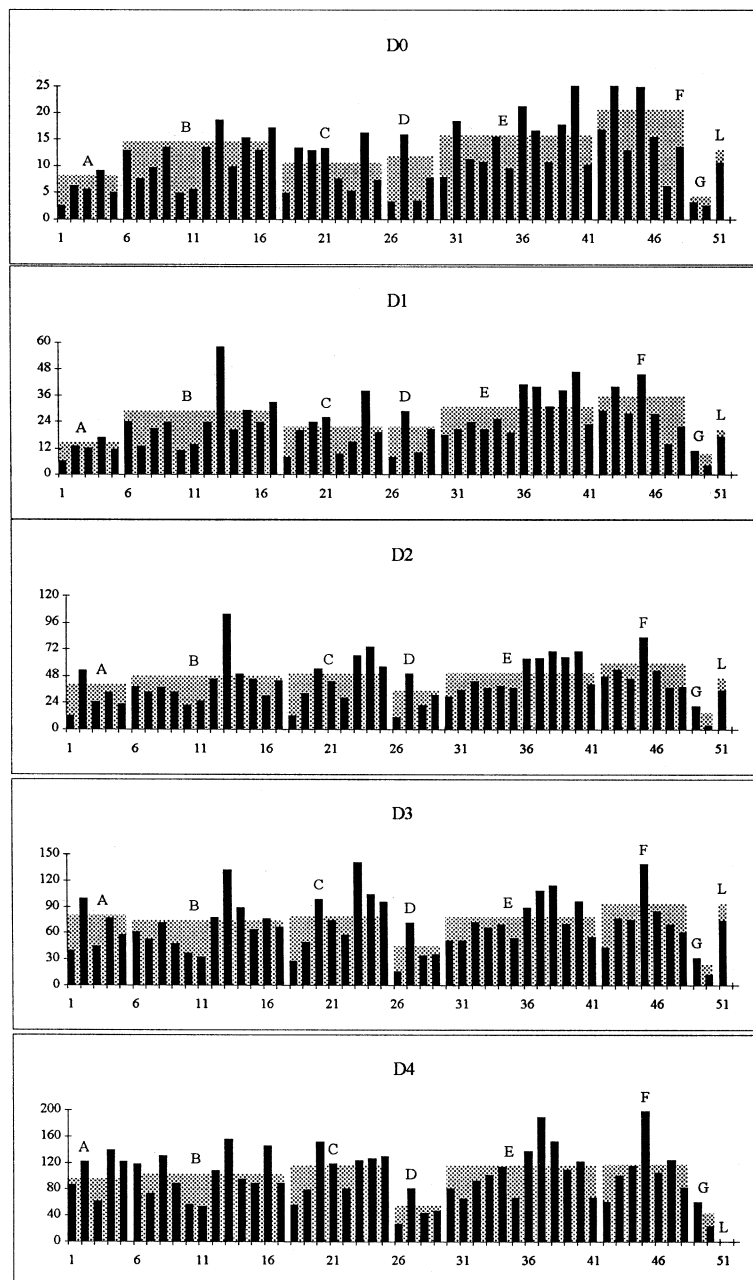
Fig. 6. Diagrams of equivalent radii D_0, D_1, D_2, D_3, D_4 of all analysed earthquakes (black histograms). In X-axis, earthquakes are labelled with identification short numbers (table III), in Y-axis the equivalent radii D_i (km) are represented. These earthquakes are grouped for similar-attenuation zones (A, B, C, D, E, F, G, L). Grey histograms indicate the equivalent radii D_i evaluated for the zones by the validation procedure.

representation it is possible to fully appreciate the quality and the heterogeneity that can be reached grouping such earthquakes, and the consequent representativeness of the average parameters set for the similar-attenuation zones. This result suggests that such analyses should be performed *a priori*, at the same time as the definition of similar-attenuation zones. It is therefore evident that it is always possible to find an average of the intensity decay but gaining validation percentages clearly smaller than those obtained before.

The radii for single earthquake were calculated with $PK = 0.5$, while the radii for the zones were computed with PK value chosen by the validation procedure. A draft average was not made (this is strongly evident for the L zone); in fact fig. 7 shows, as an example, the

attenuation curve for the D zone (bold line) and for each single earthquake of that zone. The curve for the zone tries to take in account the biggest single event establishing quite big D_i, causing a large number of *overestimated* observations, as observed in table V: here the final results are shown. The values of the elected D_i sets are represented, together with the corresponding parameters of attenuation law in the validation categories. Beside the L zone, for which only one earthquake was available and not suitable for isotropic attenuation law, the validation results show that the worst result is for D zone. For the other zones, values greater than 50% were obtained. In our opinion this is caused by the very different attenuation trend of the grouped earthquakes, as seen in fig. 7 for the D zone.
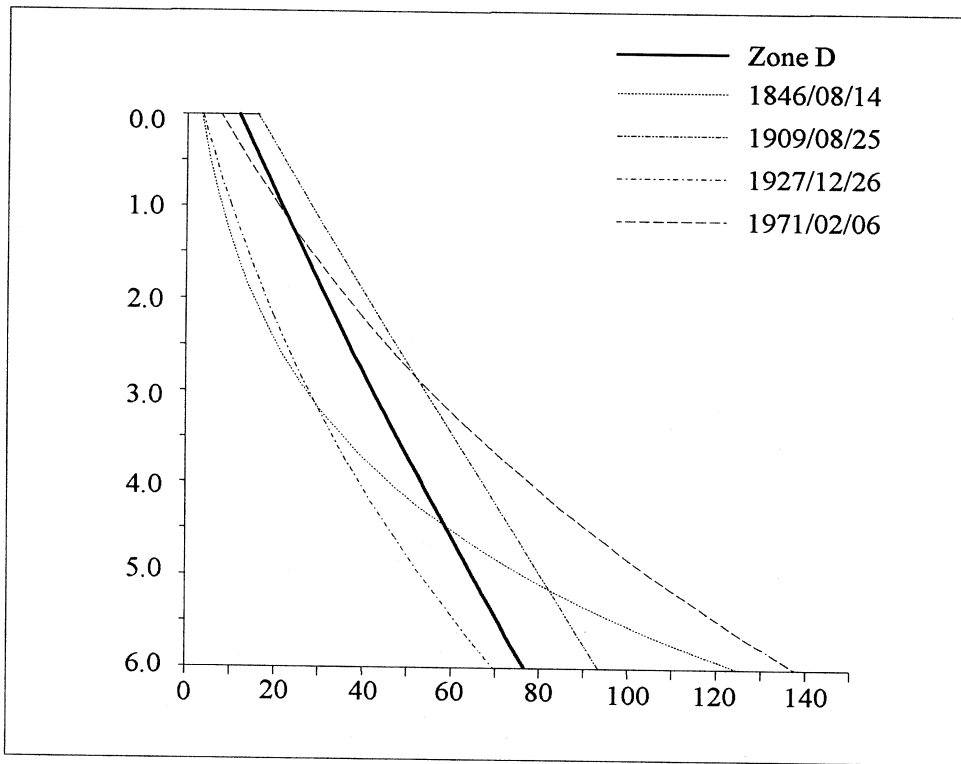

Fig. 7. Chart of intensity decay *versus* distance (km) in D zone. The bold line represents the average intensity decay evaluated for D zone. The other lines indicate the attenuation of the single analysed earthquakes (1846/08/14, I_0 = IX; 1909/08/25, I_0 = VII-VIII; 1927/12/26, I_0 = VII-VIII; 1971/02/06, I_0 = VII-VIII).
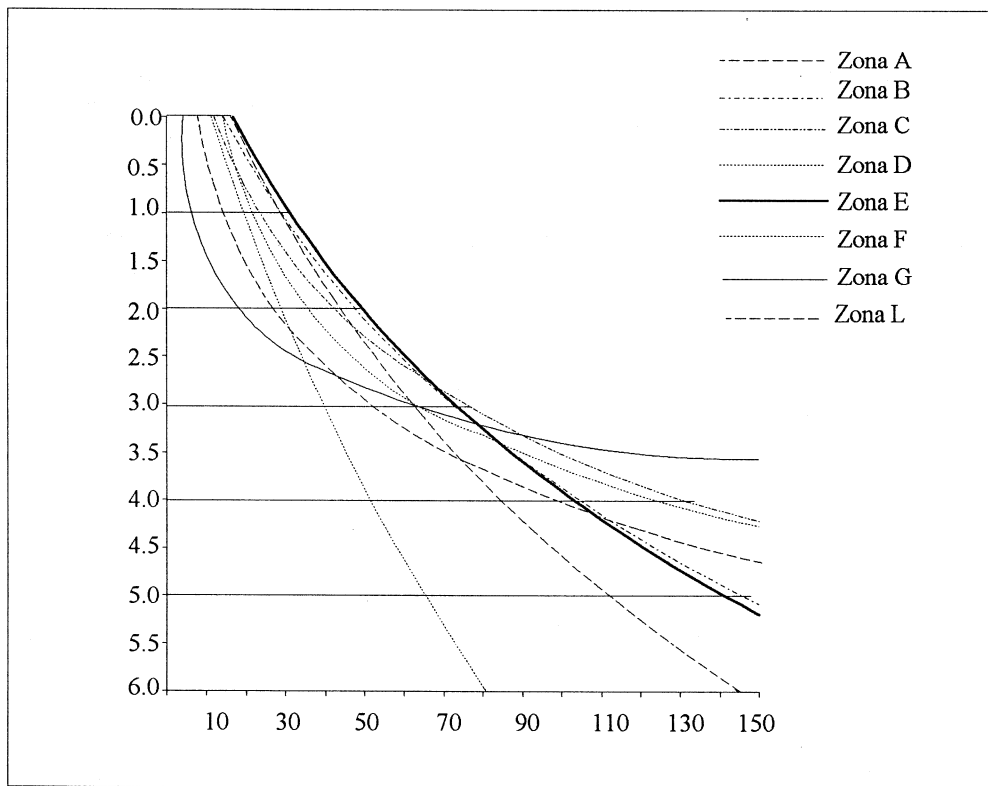
Fig. 8. Chart of intensity decay *versus* distance for similar-attenuation zones (A, B, C, D, E, F, G, L). The parameters of attenuation laws were selected by the validation procedure, analysing all the earthquakes belonging to the same zone simultaneously.

Figure 8 shows the attenuation laws selected for every similar-attenuazion zone in table V. From this graph it is evident that the laws are distinct. The G zone, where the Etna and Vesuvio volcanoes are located, shows a decay greater than other zones, as expected for a volcanic earthquake zone.

8. Conclusions

Using observed intensity data sets directly, an objective and reproducible procedure was defined to estimate the equivalent radius D_i. With these values, the parameters set of an attenuation law was defined for single earthquakes and for joined earthquakes of similar-attenuation zones. The proposed method was tested on the case study and it demonstrated, in general, a fairly good behaviour.

The parameters estimated using single earthquakes showed a good percentage of validation, whereas the average parameters obtained by analysing a set of earthquakes belonging to the same similar-attenuation zone gave a lower percentage. This is an important result since the outcome mainly required is the capability to estimate on average the intensity decay for a large zone.

Finally through the validation procedure a criterion to define the accuracy of an attenuation law is proposed: grouping data into five

classes with respect to the attenuation law capability to match the observed intensity at site, a measure of attenuation law goodness is defined.

Furthermore, the procedure proposed in this paper, applied to a larger set of earthquakes, can be combined with usual seismotectonic analysis for the definition of similar-attenuation zones with a greater number of elements.

Acknowledgements

REFERENCES

AMBRASEYS, N. (1985): Intensity-attenuation and magnitude-intensity relationships for Northwest earthquakes, in *Earthquakes Engineering and Structural Dynamics*, **13**, 733-778.

BARBANO, M.S. and G. ZONNO (1985): Determinazione dei coefficienti di attenuazione del campo macrosismico per l'area del Cansiglio Bellunese, in *Atti del 4° Convegno Annuale del Gruppo Nazionale di Geofisica della Terra Solida, Roma 29-31 ottobre 1985*, 473-487.

BLAKE, A. (1941): On the estimation of focal depth from macroseismic data, *Bull. Seism. Soc. Am.*, **31** (3), 225-232.

GNDT, GRUPPO SISMICITÀ (1994): *Extract from Seismicity Data Base of GNDT*, unpublished report.

GRANDORI, G., F. PEROTTI and A. TAGLIANI (1987): On the attenuation of macroseismic intensity with epicentral distance, in *3rd International Conference Soil Dynamics and Earthquakes Engineering, Princeton «Ground Motion and Engineering Seismology»*, edited by A.S. CAKMAK (Elsevier, Amsterdam), 581-594.

GRANDORI, G., A. DREI, F. PEROTTI and A. TAGLIANI (1991): Macroseismic intensity versus epicentral distance: the case of Central Italy, *Tectonophysics*, **193**: *Investigation of Historical Earthquakes in Europe*, 165-171.

JOHNSON, N.L. and S. KOTZ (1970): *Distributions in Statistics, Continuous Univariate Distribution*, vol. I-II (Wiley & Sons).

PETRINI, V. (Coord.) (1980): *Proposta di Riclassificazione Sismica del Territorio Nazionale*, ESA, Roma, pubblication No. 361, pp. 83.

PETRINI, V. (1995): *Pericolosità Sismica e Prime Valutazioni di Rischio in Toscana*, edizione Regione Toscana – Istituto di Ricerca sul Rischio Sismico – CNR.

SCANDONE, P. and C. MELETTI (1992): Zonazione sismotettonica, in *Corso di Formazione Rischio Sismico Regione Toscana – Giunta Regionale Dipartimento Ambiente* edited by CNR-Gruppo Nazionale per la Difesa dai Terremoti e Dipartimento di Scienze della Terra dell'Università di Pisa.

SCANDONE, P., E. PATACCA, C. MELETTI, M. BELLATALLA, N. PERILLI and U. SANTINI (1992): Struttura geologica, evoluzione cinematica e schema sismotettonico della penisola italiana, in *Atti del Convegno Annuale del Gruppo Nazionale per la Difesa dai Terremoti, Pisa, 25-27 Giugno 1990* (Tipolitografia Moderna, Bologna), 119-135.

SPONHEUER, W. (1960): Methoden zur Herdtielenbestimmung in der Makroseismik, *Freiberger Forschungsh*, C88.

TERAMO, A., E. STILLITANI and A. BOTTARI (1995): On an anisotropic attenuation law of the macroseismic intensity, *Natural Hazard*, **11** (3), 203-221.